**Project Report**
**ATC-246**

# Report on Product Performance for the Terminal Doppler Weather Radars (TDWRs) at Washington National Airport and Memphis and Orlando International Airports

**D. Klingle-Wilson**
**M. Isaminger**
**C. Keohan**

**29 January 1997**

## Lincoln Laboratory
MASSACHUSETTS INSTITUTE OF TECHNOLOGY
*LEXINGTON, MASSACHUSETTS*

Prepared for the Federal Aviation Administration,
Washington, D.C. 20591

TECHNICAL REPORT STANDARD TITLE PAGE

| 1. Report No. | 2. Government Accession No. | 3. Recipient's Catalog No. |
|---|---|---|
| ATC-246 | | |

| | |
|---|---|
| 4. Title and Subtitle<br>Report on Product Performance for the Terminal Doppler Weather Radars (TDWRs) at Washington National Airport and Memphis and Orlando International Airports | 5. Report Date<br>29 January 1997<br>6. Performing Organization Code |
| 7. Author(s)<br>D. Klingle-Wilson, M. Isaminger, C. Keohan | 8. Performing Organization Report No.<br>ATC-246 |
| 9. Performing Organization Name and Address<br>MIT Lincoln Laboratory<br>244 Wood Street<br>Lexington, MA 02173-9108 | 10. Work Unit No. (TRAIS)<br>11. Contract or Grant No.<br>DTFA01-93-Z-02012 |
| 12. Sponsoring Agency Name and Address<br>Department of Transportation<br>Federal Aviation Administration<br>Washington, DC 20591 | 13. Type of Report and Period Covered<br>Project Report<br>14. Sponsoring Agency Code |

15. Supplementary Notes

This report is based on studies performed at Lincoln Laboratory, a center for research operated by Massachusetts Institute of Technology, under Air Force Contract F19628-95-C-0002.

16. Abstract

Massachusetts Institute of Technology Lincoln Laboratory is supporting the Terminal Doppler Weather Radar (TDWR) Program Office and Program Support Facility in the performance analysis of deployed TDWR systems, and resulting recommendations for system enhancements. This report, the first of a series, documents measured performance of the TDWR at Washington National Airport (DCA), Memphis International Airport (MEM) and Orlando International Airport (MCO). Performance of the TDWR depends on optimization. Therefore, the report includes a description of the optimization procedure, using DCA as an example. For each site, the generation of clutter residue editing maps (CREMs), the collection of base data (Doppler velocity and reflectivity) and product data (algorithm detections), the assessment of the performance of the microburst and gust front detection algorithms are discussed.

To assess algorithm performance, human experts generate a data base of ground truth of microbursts and gust fronts. These data are automatically compared to algorithm detections and performance statistics are generated. Running Build 5A software at DCA, the microburst algorithm probability-of-detection (POD; 93.7 percent) met the requirement (a minimum POD of 90 percent) for the TDWR system. The probability-of-false-alarm (PFA) for the algorithm (19.7 percent) did not meet the requirement (maximum PFA of 10 percent) for the TDWR system. With the Build 5B parameters, the POD and PFA were 92.3 percent and 9.5 percent, respectively. If implemented, a test for the proximity of vertically integrated liquid water will decrease the false alarm probability further. At MEM and MCO, the microburst detection algorithm comfortably met the POD requirement with both sites exceeding 95 percent. However, both sites exceeded the PFA requirement with PFA of 11.6 percent at MCO at 12.2 percent at MEM. These sites were running Build 5A software. Analysis of algorithm performance using 5B software showed a significant decrease in PFA (to 5.5 percent at MCO and 7.4 percent at MEM) while maintaining a POD of above 93 percent.

The gust front algorithm achieved a POD of 47.3 percent for all sites and all strengths of gust fronts and a PFA of 10.5 percent for all sites. There are no formal requirements for POD and PFA for the gust front detection algorithm. Detection capability improved with gust front strength. POD for all moderate and strong gust fronts was 79.9 percent and 91.9 percent, respectively.

Based on the findings reported herein, it is recommended that the following actions be taken to improve the performance of the TDWR system:

1. The VIL test should be evaluated by the TDWR Program Support Facility as a means to further reduce the microburst/wind shear PFA, which may approach the 10 percent threshold even with the 5B software.
2. Resources permitting, the gust front algorithm should be replaced with the Machine Intelligent Gust Front Algorithm.
3. Data quality problems such as range aliasing, velocity aliasing and noise contamination should be investigated in detail to determine methods for the mitigation of these problems.
4. The scan mode switching criteria should be thoroughly evaluated to determine why the radar switches modes on reflectivity values below the threshold.

| 17. Key Words | | 18. Distribution Statement |
|---|---|---|
| Terminal Doppler Weather Radar<br>microburst detection algorithm<br>Gust Front Algorithm<br>clutter | Data quality<br>Gust Front<br>microburst<br>reflectivity | This document is available to the public through the National Technical Information Service, Springfield, VA 22161. |

| 19. Security Classif. (of this report) | 20. Security Classif. (of this page) | 21. No. of Pages | 22. Price |
|---|---|---|---|
| Unclassified | Unclassified | 42 | |

FORM DOT F 1700.7 (8-72) Reproduction of completed page authorized

# EXECUTIVE SUMMARY

Massachusetts Institute of Technology Lincoln Laboratory is supporting the Terminal Doppler Weather Radar (TDWR) Program Office and Program Support Facility in the performance analysis of deployed TDWR systems, and resulting recommendations for system enhancements. This report, the first of a series, documents measured performance of the TDWR at Washington National Airport (DCA), Memphis International Airport (MEM) and Orlando International Airport (MCO). Performance of the TDWR depends on optimization. Therefore, the report includes a description of the optimization procedure, using DCA as an example. For each site, the generation of clutter residue editing maps (CREMs), the collection of base data (Doppler velocity and reflectivity) and product data (algorithm detections), and the assessment of the performance of the microburst and gust front detection algorithms are discussed.

To assess algorithm performance, human experts generate a data base of ground truth of microbursts and gust fronts. These data are automatically compared to algorithm detections and performance statistics are generated. Running Build 5A software at DCA, the microburst algorithm probability-of-detection (POD; 93.7 percent) met the requirement (a minimum POD of 90 percent) for the TDWR system. The probability-of-false-alarm (PFA) for the algorithm (19.7 percent) did not meet the requirement (maximum PFA of 10 percent) for the TDWR system. With the Build 5B[1] parameters, the POD and PFA were 92.3 percent and 9.5 percent, respectively. If implemented, a test for the proximity of vertically integrated liquid water will decrease the false alarm probability further. At MEM and MCO, the microburst detection algorithm comfortably met the POD requirement with both sites exceeding 95 percent. However, both sites exceeded the PFA requirement with PFA of 11.6 percent at MCO and 12.2 percent at MEM. These sites were running Build 5A software. Analysis of algorithm performance using 5B software showed a significant decrease in PFA (to 5.5 percent at MCO and 7.4 percent at MEM) while maintain a POD of above 93 percent.

The gust front algorithm achieved a POD of 47.3 percent for all sites and all strengths of gust fronts and a PFA of 10.5 percent for all sites. There are no formal requirements for POD and PFA for the gust front detection algorithm. Detection capability improved with gust front strength. POD for all moderate and strong gust fronts was 79.9 percent and 91.9 percent, respectively.

Based on the findings reported herein, it is recommended that the following actions be taken to improve the performance of the TDWR system:

---

1. Early TDWR sites were fielded with a software package known as Build 5A. Build 5B is an upgraded software package containing changes to several site adaptation parameters that help to mitigate microburst algorithm false alarms. The 5B results that were evaluated in this report were generated by the 5B software running at MIT Lincoln Laboratory

1. The VIL test should be evaluated by the TDWR Program Support Facility as a means to further reduce the microburst/wind shear PFA, which may approach the 10 percent threshold even with the 5B software.

2. Resources permitting, the gust front algorithm should be replaced with the Machine Intelligent Gust Front Algorithm.[2]

3. Data quality problems such as range aliasing, velocity aliasing and noise contamination should be investigated in detail to determine methods for the mitigation of these problems.

4. The scan mode switching criteria should be thoroughly evaluated to determine why the radar switches modes on reflectivity values below the threshold.

---

2. An improved gust front detection algorithm as described by Troxel and Delanoy, 1994.

# TABLE OF CONTENTS

# TABLE OF CONTENTS (CONTINUED)

# LIST OF FIGURES

# LIST OF TABLES

# 1. INTRODUCTION

Massachusetts Institute of Technology Lincoln Laboratory provides support to the Terminal Doppler Weather Radar (TDWR) Program Office in the performance analysis of deployed TDWR systems, and resulting recommendations for system enhancements. This report documents initial performance of the TDWR products at Washington National Airport (DCA), Memphis International Airport (MEM) and Orlando International Airport (MCO). This performance depends, in turn, on the site optimization performed for the specific radars. Therefore, an overview of site optimization process, using DCA as a concrete example, is included.

After the sites were optimized, base data (Doppler velocity and reflectivity) and product data (algorithm detections) were collected to assess the quality of the base data and the performance of the microburst and gust front detection algorithms. It is assumed that the reader of this report has an extensive knowledge of the TDWR system. An overview of the wind shear detection capabilities of the TDWR can be found in Merritt, *et al.* (1989).

# 2. SITE OPTIMIZATION

Site optimization consists of verifying that the site adaptation parameters are set correctly, calibrating the radar, fine-tuning the scan strategy, and generating clutter residue editing maps (CREM). Calibration of the radar includes verifying the location of the moving target simulator (MTS) and the elevation angle (or tilt) and azimuth alignment by comparing the known position of the sun with the position as estimated by the antenna. The MTS is used as an end-to-end test to verify that the radar transmitter, antenna, receiving chain, and data processor produce correct Doppler velocity and reflectivity estimates.

## 2.1 Site Adaptation Parameters

The DCA site was optimized on 13 November 1995 by Mark Isaminger of Massachusetts Institute of Technology Lincoln Laboratory and Keith Aclin of the TDWR Program Support Facility, working with the Federal Aviation Administration Airways Facilities and Sector Field Office personnel. The site adaptation parameter set was verified, including the MTS magnetic azimuth. The microburst velocity signal-to-noise ratio (SNR) is used to reject Doppler velocity estimates that may not be accurate. Velocity estimates that are associated with SNRs that are below the site-adaptable parameter value are not used by the detection algorithm. The nominal values for the microburst velocity SNR are listed in Table 1. The SNR parameter chosen for DCA is 8 dB.

**Table 1**

**Microburst Velocity Signal-to-Noise Ratio**

| Region | SNR (dB) |
|---|---|
| Western Plateau | 6 |
| Florida, Gulf Coast, Puerto Rico | 10 |
| Default | 8 |

## 2.2 MTS Location

The MTS is used to align the antenna and calibrate the radar. The location of the MTS is known and is scanned by the antenna. The location of the MTS as identified in the radar data is compared to the known location of the MTS and, if necessary, the alignment of the antenna is adjusted so that the sensed location and known location coincide. The site adaptable parameter settings for the location of the MTS at DCA are provided in Table 2.

**Table 2**

**Moving Target Simulator Parameter Settings**

| Parameter | Value |
|---|---|
| Azimuth (magnetic) | 20.4° |
| Range Cell | 71 |
| Elevation angle | 0.2° |

## 2.3 Antenna Alignment

When the antenna is pointing at the MTS, the reflectivity value at the MTS location should be within ± 3 dB of 50 dBZ. The MTS velocity should be between –4.978 m/s and –5.021 m/s. The alignment data for DCA are provided in Table 3.

A sun tracking program is used to fine-tune the alignment of the TDWR antenna. The program is run once in the morning and once in the afternoon. The antenna is pointed to the known location of the sun. The sun's signal level is measured and compared to the expected signal level. Differences between the expected and measured signal levels are used to compute the azimuth and elevation angle alignment errors. If the elevation and/or azimuth angle error is greater than a tenth of a degree, a program is run to determine the offset settings required to correct the errors.

**Table 3**

**Moving Target Simulator Alignment Data**

| Parameter | Value |
|---|---|
| MTS Reflectivity | 51.5 dBZ |
| MTS Velocity | –4.98 m/s |

The sun track showed that the azimuthal offset for the DCA site is 0.1072°, which is considered insignificant since the azimuth resolution of the system is one degree. The elevation offset is 0.0412° and the total beam error after correction is 0.1149°.

### 2.4 Scan Strategy

The TDWR uses two scan modes: Monitor and Hazardous. Monitor mode is used in the absence of significant weather (as defined in Table 6) to reduce wear on the TDWR hardware. Monitor mode consists of a series of full 360-degree sweeps at different elevation angles. Hazardous mode is used in the presence of significant weather to detect microbursts and wind shears in a timely fashion. Hazardous mode consists of a combination of full-circle sweeps and sector sweeps at various elevation angles. The Hazardous mode and Monitor mode scan strategies for DCA are provided in the Appendix. The azimuthal limits of the sector sweeps are from 267° clockwise to 27°. The surface elevation scan for microburst detection at DCA is verified as 0.3°.

### 2.5 Clutter Suppression and Editing

Clutter suppression filters are used to remove ground clutter from the radar data. A clutter suppression filter is matched to a range of operational pulse repetition intervals (PRI). The operational PRI is selected based on the typical operational PRI while scanning in hazardous mode. The default value of the operational PRI is 798 microseconds (pulse repetition frequency, or PRF, of 1253 pulses per second). Filter number 2 is matched to this PRI and is therefore the default filter number. Whenever possible, the clutter maps are generated from data collected with the default filter and PRI. On the day that DCA was optimized, out-of-trip contamination was present when using the default PRI. Due to the potential contamination from out-of-trip echoes, the DCA clutter data were collected using a PRI of 678 (PRF of 1475). The filter that matches this PRI is filter number 3.

Clutter suppression filters are not entirely successful at removing all ground clutter. Heavy fixed clutter and clutter from moving objects are not fully suppressed. To suppress the remaining (residual) clutter, CREMs are used to edit the incoming data. These maps contain a characteristic reflectivity for each gate. During operations, incoming data are compared gate-by-gate to the appropriate CREM value. Any reflectivity in the incoming data that does not exceed the CREM reflectivity plus the Clutter Breakthrough Threshold (which accounts for the inherent variability of ground clutter) is assumed to be ground clutter and is removed.

CREM measurements are made on clear-air days when anomalous propagation (AP) is not occurring. Detection of low reflectivity wind shear events requires that the TDWR be capable of measuring Doppler wind velocities in clear air conditions. In the absence of reflectivity from in-trip and out-of-trip weather and AP, the echoes in the CREMs are due entirely to ground clutter residue and clear-air returns. In order to avoid removing clear air returns as clutter residue, gates whose apparent clutter residue levels do not exceed the expected clear-air reflectivity (CAR) are not clutter-residue edited.

Prior to collecting clutter data for the CREMs, it is essential that the clutter suppression levels provided by the clutter filters be verified. This is accomplished by running a certification program on the receiver, transmitter, and signal processor chain of both radar channels. Certification requires an analysis of the pilot pulse. The pilot pulse provides a stability measurement of the transmitted and received pulse. The certification values for both channels of the DCA TDWR are provided in Table 4. The nominal value for both channels

**Table 4**

**Clutter Suppression Levels (dB) for Channels A and B**

| | Channel A (dB) | Channel B (dB) |
|---|---|---|
| Filter 1 | 52.3 | 54.2 |
| Filter 2 | 52.9 | 53.3 |
| Filter 3 | 52.9 | 53.6 |
| Filter 4 | 53.8 | 53.3 |

with all filters is 54 dB. The certification performed at DCA on 13 November 1995 indicated that the clutter suppression levels were within tolerance (within 2 dB of 54 dB).

After verifying the adaptation parameters, system alignment, and calibration, a low elevation scan is performed to ensure that conditions are sufficient for generating a good CREM (i.e., no AP or out-of-trip echoes). The first step in generating a CREM is to estimate the CAR value. CAR is calculated using a specially designed scan strategy composed of tilts from 2.0° to 30.0°. Clear air samples are collected over ranges of 1 to 10 km from the radar and over altitudes of 0.1 to 0.5 km above ground level (AGL). A histogram is computed from 10,000 valid samples. The CAR value is taken as the ninetieth percentile of the distribution. The maximum allowable reflectivity for a clear air sample is 30 dBZ; the minimum allowable radial velocity is 3 m/s. The CAR value for the subject DCA optimization was −1.5 dBZ.

CREMs are generated by performing multiple scans at the lowest tilts under clear air conditions. CREMs are generated for each tilt that contains significant clutter residue. The CREM generation scan is run until the desired number of valid samples (e.g., 21) are collected for each range sampling volume (gate). Using these data, the ground clutter reflectivity within each gate is computed as the average of the samples. The base data display (BDD) is used to verify visually there is no contamination of the clutter maps by anomalous propagation or out-of-trip echoes. The resulting CREMs are installed as system default maps for both Hazardous and Monitor scan modes. Finally, the radar is scanned in both hazardous and monitor modes to confirm that the CREMs are implemented on the correct tilts.

It is possible to manually edit and override map values in order to alter the map features. For example, moving vehicles on highways can be a significant clutter source that is not handled well by the clutter residue editing technique. The CREM can be modified to account for this clutter source by the use of editing polygons. Using the BDD, the region to be edited via polygons is identified and the coordinates of the polygon are determined. All of the CREM values inside the polygon are set to the desired reflectivity value. If weather reflectivities exceed the polygon value, the weather data are passed through. One polygon was used to edit the DCA CREM to account for a high-reflectivity clutter source near the airport which remained after the initial CREM was applied.

The parameters used to generate the clutter residue maps for DCA are provided in Table 5. For DCA, CREMs were created for the 0.3° and 1.0° tilts. The PRF/filter combination was chosen to represent the ideal operational PRFs of the system under hazardous mode scanning conditions. The Clutter Breakthrough Parameter is the reflectivity value which is added to the CREM value to account for scan-to-scan clutter variability, nominally 8 dB. Ground clutter may display a velocity signature due to feedhorn motion, clutter filtering or contamination from vehicles and birds. The nominal maximum radial velocity threshold (10 m/s) allows the velocity of clutter to be as much as 10 m/s. Due to the presence of out-of-trip weather in the DCA map, the maximum radial velocity threshold was lowered to 5 m/s so out-of-trip weather would not be included in the CREM as clutter. A nominal velocity threshold of 10 meters per second is not appropriate

**Table 5**

**Parameters Used to Generate Clutter Residue Editing Maps for DCA**

| Parameter | Value |
|---|---|
| Channel | A |
| PRF (pulses per second) | 1474.9 |
| PRI (microseconds) | 678 |
| Filter | 3 |
| Clutter Breakthrough Parameter (dB) | 8 |
| Maximum Radial Velocity (m/s) | 5 |

to distinguish clutter residue from weather or out-of-trip weather. Thus, a more detailed analysis should be performed by collecting clutter data with different velocity thresholds to determine the most appropriate default value. The resulting CREM for the 0.3° tilt is shown in Figure 1.

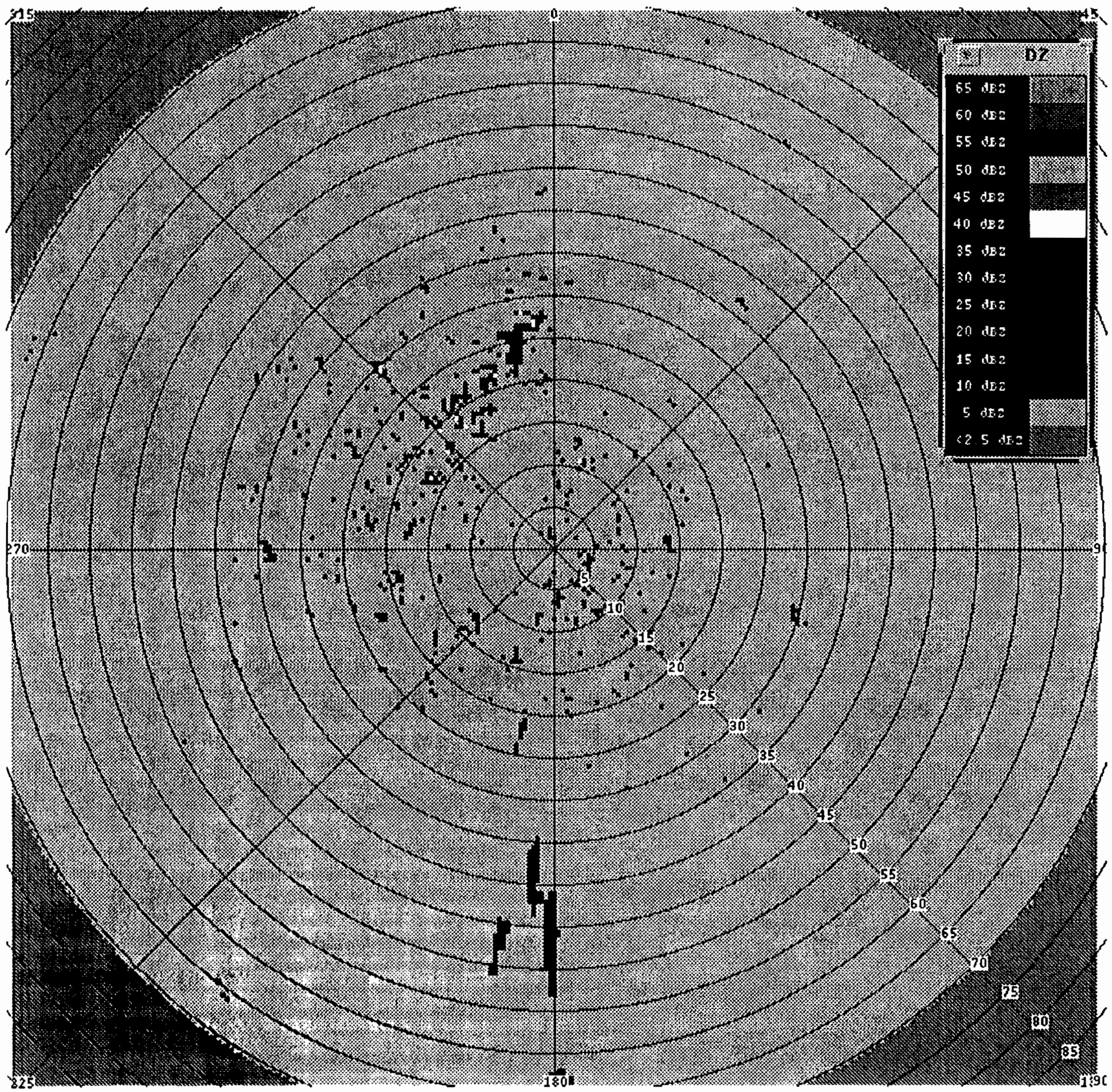


*Figure 1. CREM for the 0.3° elevation angle at DCA. The high reflectivity values at the 180° azimuth is contamination due to out-of-trip weather.*

# 3. DATA COLLECTION

Two types of data are collected at each TDWR site; base data and product data. Base data are comprised of the radial-by-radial, gate-by-gate reflectivity and Doppler velocity data. Product data are comprised of the algorithm outputs that are sent to the display functional unit (DFU), including microburst shapes, gust front detections and forecasts, precipitation levels, and messages to be written to the Ribbon Display Terminal.

Base data are collected by installing an ethernet board into the Harris Radar Product Generator (RPG). Figure 2 provides a schematic of the recording system. The base data are transferred from the RPG to a recorder (a 10-cassette jukebox) via ethernet. To collect TDWR product data, a Y-cable is attached to the port that provides input to the BDD. Product data are read from the BDD input stream and sent to a Lincoln Laboratory Sun workstation for recording.

A data recorder was installed at the DCA site and base data collection began 24 August 1994. Base data were recorded when the radar scanned in Hazardous mode. On 15 December 1994, the recording software was upgraded to record base data when the radar scans in Monitor mode AND if a microburst and/or gust front detection is declared, in addition to the Hazardous mode recording. Base data recording stopped on 8 February 1995, due to hardware problems at the DCA site and the installation of software that does not support the ethernet connection. In DCA, product data were recorded not from the BDD, but from the DFU port. The product data were collected continuously from 1 September 1994 until 20 January 1995 when the DFU at the radar shelter was removed.

During 1994 and 1995, TDWR base and products data were collected at both MEM and MCO in support of the Integrated Terminal Weather System (ITWS) prototype testing at these sites. Because these sites are staffed, the recording procedure was slightly different than at DCA. The recording hardware (e.g., Sun Workstation and jukebox recorder) were located at the ITWS site instead of the TDWR. The base data were received from the Harris via a T1 digital data line, while the products data were acquired from the DFU over a 56 kilobaud digital data line. The TDWR recording processes were started whenever ITWS was operational. In general, the processes were started prior to the formation of weather in the area. Thus, at the ITWS sites data were collected in both Monitor and Hazardous modes, regardless of a gust front or microburst detection.

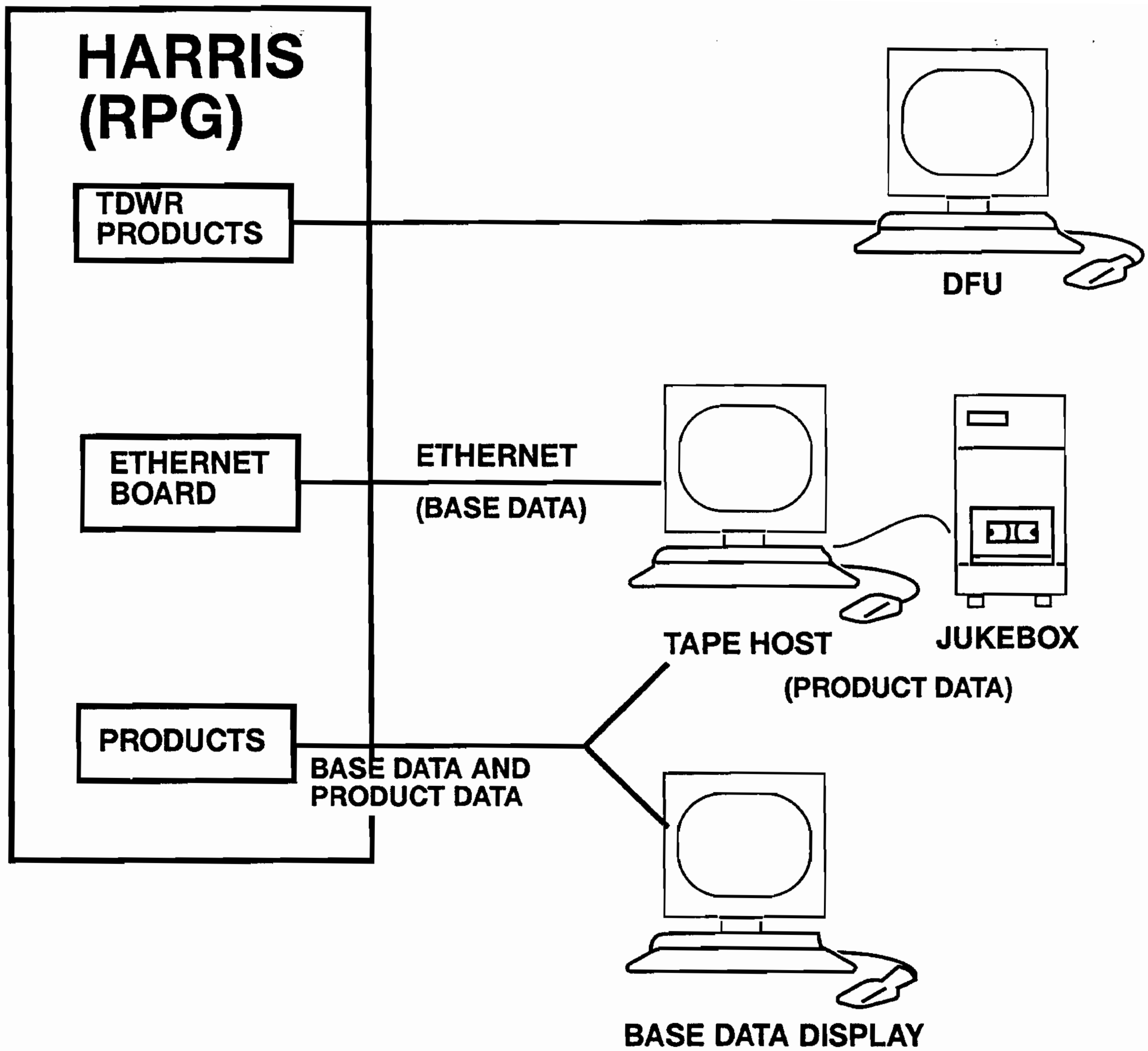


*Figure 2 . Schematic diagram of data collection process.*

# 4. BASE DATA ASSESSMENT

## 4.1 Automatic Scan Mode Switching

Early TDWR sites were fielded with a software package known as Build 5A. An upgrade to this software package known as Build 5A, version 27 (5A.27) contained changes to several site adaptation parameters that control automatic scan mode switching. A comparison of the Build 5A and 5A.27 parameters relative to automatic scan mode switching are presented in Table 6.

**Table 6**

**Comparison of Build 5A and Build 5A, Version 27 Parameters for Automatic Scan Mode Switching**

| Parameter | Build 5A | Build 5A.27 |
|---|---|---|
| **Monitor to Hazardous** | | |
| Minimum Reflectivity (dBZ) | 20 | 30 |
| Minimum Number of Contiguous Gates | 33 | 13 |
| Minimum Altitude (km AGL) | 2 | 2 |
| **Hazardous to Monitor** | | |
| Minimum Time after Last Detection (min) | 30 | 30 |

Base data were perused to identify possible problems. First, the data are examined to determine if the system automatically switches scan modes correctly. The TDWR radar is designed to automatically switch from Monitor mode to Hazardous mode if a gust front, microburst, or significant reflectivity feature is detected within the TDWR sector and within 45 km of the airport reference point. In Build 5A, a significant reflectivity feature is defined as a region of at least 33 contiguous gates (Minimum Number of Contiguous Gates) containing reflectivities of at least 20 dBZ (Minimum Reflectivity) above an altitude of 2 km (Minimum Altitude). The radar switches from Hazardous to Monitor mode 30 minutes after the last microburst, gust front, or significant reflectivity feature is detected (Minimum Time after Last Detection).

It appears that the DCA TDWR radar spent excessive time in Hazardous mode due to inadequate editing of out-of-trip echoes above 2 km AGL and due to gust front algorithm false alarms. In addition, the radar switched to Hazardous mode properly when the reflectivity threshold was exceeded in stratiform precipitation conditions, which are unlikely to produce wind shears. The mode switching on many of the stratiform rain and out-of-trip cases was caused by the Minimum Reflectivity threshold setting of 20 dBZ in Build 5A. The Build 5A.27 value for this parameter is 30 dBZ, which should help to alleviate the problem. Due to the recent failures of the antenna components at most TDWR sites, decreasing the time spent in Hazardous mode during weather conditions not conducive to producing wind shear should help extend the lifetime of the hardware. In addition, it is worth considering an alternative hazardous scan strategy that minimizes or eliminates the number of sector scans performed by the antenna.

Data collected in Memphis during 1995 showed that even with the 5A.27 parameter set the radar switched into Hazardous mode on reflectivity cells that were below the 30 dBZ threshold. The parameters were verified as correct and it was confirmed that the automatic switching algorithm used fully conditioned reflectivity data. Therefore, the cause of these inadvertent switches is unknown and needs to be investigated.

### 4.2 Data Quality

Other problems that were identified using the base data were dealiasing failures and out-of-trip contamination due to the fast moving storm systems. Rings of missing data (e.g., from several gates to 1 km in range extent) were observed also. An analysis of the low PRF data for these cases showed the range obscuration algorithm might be processing the last three range gates, which are used for Digital Signal Processor diagnostics. Due to the diagnostics, the data in these gates might be contaminated and have high signal-to-noise ratios. The range obscuration algorithm assumes these data are valid weather signals and edits the in-trip signal accordingly. If this is the case, the algorithm should be changed to ignore the data in the last three gates.

Another problem identified in the base data was contamination by AP-induced ground clutter breakthrough in the early morning hours. The AP conditions served to enhance the ground clutter returns that lead to an extremely noisy velocity field in the low reflectivity clear air returns. (The level of the AP before and after input to the clutter filters was 40 to 65 dBZ and 0 to 25 dBZ, respectively.) The noisy velocity field was responsible for corrupting the wind field model[3] used to dealias Doppler velocities. The gust front algorithm false alarm probability increases as a result of dealiasing failures. Velocity dealiasing errors caused by a corrupted wind field model are a major concern at those TDWR sites characterized by high winds and fast-moving storms.

3. The wind field model provides an estimate of the wind speed and direction that is used to determine when velocity aliasing is occurring and how to dealias those velocities.

# 5. ALGORITHM PERFORMANCE

## 5.1 Microburst Detection

The performance of the Microburst Detection algorithm is assessed using the metrics of probability of detection (POD) and probability of false alarm (PFA). POD is defined as the number of correct detections divided by the number of true events. PFA is defined as the number of detections not supported by truth divided by the total number of algorithm detections. For a detection to be considered correct, the detection must overlap a true event by at least 25 percent. Any detection that does not overlap an event by at least 25 percent is considered a false alarm. Any event that is not overlapped by at least 25 percent of a detection is considered a miss.

Microburst truth data are generated by a human expert. Divergence signatures are identified in the TDWR Doppler velocity data. The differential Doppler velocity across the outflow must equal or exceed 10 m/s over a maximum of 4 km in range extent somewhere within the event. The reflectivity field is examined to verify that the signature is within a storm echo. The location and intensity of the divergences are entered into an on-line data base to support automated comparison with algorithm detections.

The TDWR software contains numerous parameters that affect the performance of the wind shear/microburst detection algorithm. A comparison of some of those parameters for Build 5A and 5B[3] are provided in Table 7. The Minimum Divergence Segments parameter is the minimum number of segments required to define a divergence region. This region may become a microburst detection if it overlaps a microburst feature aloft and the divergence is greater than 10 m/s. The Minimum Alarm Segments parameter is the minimum number of alarm segments used to define a new microburst/wind shear event, based on an overlap with a divergence region from a surface tilt during the previous two minutes. The Minimum Alarm DeltaV is the minimum velocity differential needed to define a microburst/wind shear event. The Minimum Storm Top Altitude parameter is the minimum altitude a storm top feature must be for a reflectivity feature to be considered a true storm. The Storm Centroid Distance is the maximum distance a microburst/wind shear alarm may be from a storm centroid in order to be considered valid. The Storm Overlap Threshold Test (available only in Build 5B) parameter is the maximum distance the microburst/wind shear alarm centroid may be from a storm cell bounding box in order to be considered valid. A Storm Overlap Threshold Test value of 0 km means that the alarm and bounding box must touch or overlap.

3. Build 5B is a software upgrade from Build 5A and its various versions. Build 5B contained several changes to site adaptation parameters that help to mitigate microburst algorithm false alarms.

**Table 7**

**Comparison of Build 5A and Build 5B Parameters for Microburst/Wind Shear Detection**

| Parameter | Build 5A | Build 5B |
|---|---|---|
| Minimum Divergence Segments | 3 | 4 |
| Minimum Alarm Segments | 4 | 5 |
| Minimum Alarm DeltaV (m/s) | 7.5 | 10.0 |
| Minimum Storm Top Altitude (km AGL) | 2 | 1.5 |
| Storm Centroid Distance (km) | 20 | 3 |
| Storm Overlap Threshold Test (km) | - | 0 |

The performance requirements for the TDWR microburst algorithm are a minimum POD of 90 percent and a maximum PFA of 10 percent. Algorithm performance at DCA was determined using data from 9 days. Table 8 provides a synopsis of the data used to assess microburst algorithm performance. Based on these data, the POD for the microburst algorithm with the Build 5A parameters is 93.7 percent, which exceeds the required 90 percent. The PFA is 19.7 percent, which does not satisfy the requirement of less than or equal to 10 percent. An analysis of the false alarms showed that many of them were located outside the storm boundary and would be removed by a more stringent storm cell test.

The high false alarm probability at DCA is similar to previous scoring results (Vasiloff, 1993) with the Build 5A parameter settings. Most of the false alarms were due to data contamination or noisy velocities at the edges or outside of the storms. An analysis of the intensity of the false events revealed the majority were categorized as wind shears with a loss of 15 to 25 knots. Thus, the PFA for microburst-strength detections would be lower. Algorithm performance was re-evaluated using the Build 5B parameters listed in Table 7 in conjunction with the 5B software running at MIT Lincoln Laboratory. The PFA decreased to 9.5 percent with only a slight reduction in the POD from 93.7 percent to 92.3 percent. With the Build 5B parameters, the PFA for DCA meets the operational requirements by 0.5 percent. The implementation of a test for the proximity of vertically integrated liquid water (i.e., VIL test) should serve to decrease the false alarm probability further.

Table 8 provides performance statistics for the microburst detection algorithm using five days of Orlando data and eight days of Memphis data. Build 5A software was running at both of these sites during the time period that data were collected. The PODs for these sites were 96.4 and 95.7 percent, respectively; slightly better than the results from DCA. At both sites, the PFA exceeds the 10 percent requirement with

## Table 8

### Microburst Algorithm Performance Statistics for Washington National Airport

| | No. Detected | | No. Missed | | No. False | | POD (percent) | | PFA (percent) | |
|---|---|---|---|---|---|---|---|---|---|---|
| DATE | 5A | 5B | 5A | 5B | 5A | 5B | 5A | 5B | 5A | 5B |
| 08/26/94 | 81 | 81 | 6 | 6 | 3 | 3 | 93.1 | 93.1 | 3.6 | 3.6 |
| 09/15/94 | 0 | 0 | 0 | 0 | 6 | 1 | - | - | 100.0 | 100.0 |
| 09/22/94 | 13 | 13 | 2 | 2 | 8 | 4 | 86.7 | 86.7 | 38.1 | 23.5 |
| 09/26/94 | 123 | 121 | 8 | 10 | 32 | 13 | 93.9 | 92.4 | 20.6 | 9.7 |
| 09/27/94 | 247 | 243 | 17 | 21 | 40 | 16 | 93.6 | 92.0 | 13.9 | 6.2 |
| 10/01/94 | 4 | 4 | 0 | 0 | 12 | 3 | 100.0 | 100.0 | 75.0 | 42.9 |
| 11/01/94 | 122 | 124 | 8 | 6 | 13 | 8 | 93.8 | 95.4 | 9.6 | 6.1 |
| 11/06/94 | 0 | 0 | 0 | 0 | 4 | 3 | - | - | 100.0 | 100.0 |
| 11/21/94 | 19 | 14 | 0 | 5 | 31 | 12 | 100.0 | 73.7 | 62.0 | 46.2 |
| TOTALS | 609 | 600 | 41 | 50 | 149 | 63 | 93.7 | 92.3 | 19.7 | 9.5 |

the 5A parameter set (e.g., 11.6 percent for MCO and 12.2 percent for MEM). Using the 5B parameters, the PFA at both sites meets the requirement. The addition of the 5B parameters resulted in a two percent reduction of POD at MEM and MCO. Even so, the POD at both sites still exceeds the 90 percent performance requirement.

The quality and acceptability of the microburst algorithm performance in the TDWR system requires that the number of false alarms be low. False alarms not associated with a reflectivity structure were an early concern at the TDWR sites commissioned with 5A software. There were several cases of microburst algorithm false alarms caused by birds that roost in the vicinity of the Memphis airport. Many of these false alarms are removed with the 5B parameters, because they were located outside the reflectivity echo. However, the statistics show a slight reduction in the POD when using the 5B parameters. Analysis has shown that most of the dropped detections were classified as wind shears. Thus, the detection of microburst-strength events is not be altered with these changes. In addition, the wind shears that were removed typically very

Table 9

Microburst Algorithm Performance Statistics for MCO and MEM

| | No. Detected | | No. Missed | | No. False | | POD (percent) | | PFA (percent) | |
|---|---|---|---|---|---|---|---|---|---|---|
| DATE | 5A | 5B | 5A | 5B | 5A | 5B | 5A | 5B | 5A | 5B |
| **MCO** | | | | | | | | | | |
| 07/16/94 | 206 | 199 | 4 | 11 | 18 | 10 | 98.1 | 94.8 | 8.0 | 4.8 |
| 07/18/94 | 393 | 390 | 12 | 15 | 75 | 14 | 97.0 | 96.2 | 16.0 | 3.5 |
| 08/05/94 | 198 | 190 | 7 | 15 | 12 | 5 | 96.5 | 92.7 | 5.7 | 2.6 |
| 08/06/94 | 212 | 212 | 13 | 13 | 30 | 19 | 94.2 | 94.2 | 12.4 | 8.2 |
| 08/17/94 | 78 | 76 | 5 | 7 | 8 | 0 | 93.9 | 91.6 | 9.3 | 0.0 |
| MCO TOTALS | 1087 | 1067 | 41 | 61 | 143 | 62 | 96.4 | 94.6 | 11.6 | 5.5 |
| **MEM** | | | | | | | | | | |
| 04/26/94 | 352 | 348 | 11 | 15 | 60 | 38 | 97.0 | 95.9 | 14.6 | 9.8 |
| 04/27/94 | 86 | 85 | 5 | 6 | 8 | 4 | 94.5 | 93.4 | 8.5 | 4.5 |
| 06/03/94 | 91 | 87 | 8 | 12 | 15 | 5 | 91.9 | 87.8 | 14.1 | 5.4 |
| 06/16/94 | 123 | 123 | 6 | 6 | 9 | 4 | 95.3 | 95.3 | 6.8 | 3.2 |
| 06/22/94 | 165 | 160 | 8 | 13 | 2 | 2 | 95.4 | 92.5 | 1.2 | 1.2 |
| 06/26/94 | 122 | 118 | 7 | 11 | 35 | 15 | 94.6 | 91.5 | 22.3 | 11.3 |
| 06/30/94 | 81 | 78 | 9 | 12 | 20 | 9 | 90.0 | 86.7 | 19.8 | 10.3 |
| 07/04/94 | 155 | 152 | 7 | 10 | 21 | 15 | 95.7 | 93.8 | 11.9 | 9.0 |
| MEM TOTALS | 1175 | 1151 | 61 | 85 | 170 | 92 | 95.0 | 93.1 | 12.6 | 7.4 |
| SITE TOTALS | 2262 | 2218 | 102 | 146 | 313 | 154 | 95.7 | 93.8 | 12.2 | 6.5 |

small events located on the edge of the sector or in close proximity to the radar. The algorithm detection performance for the events that impact the runway ARENAs will not be degraded with the 5B parameters.

### 5.2 Gust Front Detection

Two different metrics are used to assess how well the locations of gust fronts are reported by the algorithm. The first measure is a crude hit/miss statistic that counts a detection successful if any part of the detection overlaps a 5-km wide gust front truth region identified by a human analyst. A detection is counted as false if it falls completely outside of any truth regions. An overall POD is computed by dividing the number of successfully detected fronts by the number of fronts identified by the human analyst. The PFA is the number of false detections divided by the total number of detections (both valid and false).

The second metric better quantifies detection quality by comparing the length of the front detected by the algorithm against the total length of the region identified by the human analyst. The percent of length detected (PLD) is the length detected expressed as a percent of the length delimited by the human analyst. The percent of false length detected (PFD) reflects the fraction of total detection length that was not verified by truth. Scoring procedures for gust front position is described in more detail in Klingle-Wilson *et al.*, 1992.

Gust front truth data are generated by a human expert. To be entered into the truth data base, a gust front must exhibit a minimum radial convergence of 5 m/s over 2 km, and a length of at least 10 km. Other phenomena, such as vertical wind shear, meet these criteria but are not entered into the data base. If these phenomena are detected by the algorithm, they are scored as false alarms. Gust fronts are categorized by strength, which is determined by the change in Doppler velocity (DV) across the gust front. DV for a weak gust front is 5 to less than 10 m/s, 10 to less than 15 m/s for moderate, and 15 to less than 25 m/s for strong gust fronts.

Table 10 summarizes gust front detection performance for the TDWR gust front detection algorithm for the DCA, MCO, and MEM cases. The numbers in parentheses are the numbers used to compute the probabilities, as defined above. These numbers are provided to show the size of the database used to generate the statistics. While there are no formal requirements on the detection capability of the gust front algorithm, the performance of the algorithm for moderate and strong gust fronts is respectable. Weaker gust fronts are not detected consistently. Some gust fronts are missed because of the inability of the algorithm to detect gust fronts that present a poor viewing angle to the radar (i.e., the gust front is aligned along a radial). For example, at DCA the radar is located south-southeast of the airport and many fronts cross the airport from the west. As gust fronts move across the airport, they become radially aligned with respect to the TDWR radar and their detections are dropped. Therefore, gust fronts oriented north-south on the airport are not detected well.

**Table 10**

**TDWR Gust Front Detection Algorithm Performance Statistics**

| Strength | POD (percent) | PFA (percent) | PLD (percent) | PFD (percent) |
|---|---|---|---|---|
| **DCA** | | | | |
| Weak | (135/238) 56.7 | - | (2335/6813) 35.4 | - |
| Moderate | (84/97) 86.6 | - | (2389/5055) 47.7 | - |
| Strong | (12/13) 92.3 | - | (586/889) 66.2 | - |
| All DCA | (231/348) 66.4 | (60/333) 18.0 | (5310/12757) 42.3 | (2064/11454) 18.0 |
| **MCO** | | | | |
| Weak | (271/735) 36.9 | - | (5349/27671) 19.4 | - |
| Moderate | (32/38) 84.2 | - | (765/1351) 56.5 | - |
| All MCO | (303/773) 39.2 | (6/290) 2.1 | (6114/29022) 21.1 | (578/10717) 5.4 |
| **MEM** | | | | |
| Weak | (261/695) 37.6 | - | (4518/22289) 20.6 | - |
| Moderate | (115/154) 74.7 | - | (2702/5150) 52.3 | - |
| Strong | (45/49) 91.8 | - | (1455/2154) 67.5 | - |
| All MEM | (421/898) 46.9 | (50/484) 10.3 | (8675/29593) 29.7 | (4500/25096) 17.9 |
| All Weak | (667/1668) 40.0 | - | (12202/56773) 21.5 | - |
| All Moderate | (231/289) 79.9 | - | (5856/11556) 50.7 | - |
| All Strong | (57/62) 91.9 | - | (2041/3043) 67.1 | - |
| All Sites | (955/2019) 47.3 | (116/1107) 10.5 | (20099/71372) 28.2 | (7142/47267) 15.1 |

Another reason for misses is the vertical correlation required on the 0.3° and 1.0° tilts for gust fronts shorter than 15 km. Numerous fronts were partially detected or missed entirely because the gust front was shallow and not sensed by the 1.0° tilt. Other reasons for misses include range obscuration editing in the region of the front and weak signals at ranges greater than 35 km, resulting in a velocity void region ahead of the front and an inability to compute convergence.

The false alarms were due primarily to the lack of overlap of the gust front signature on the 0.3° and 1.0° tilt. The declared detection is an average of the signature positions on both tilts. Truth is generated by using the 0.3° tilt, since this tilt is most likely to define the location of the surface wind shear. If the 0.3° and 1.0° signatures do not overlap well because the leading edge of the gust front slopes with height, the resulting detection does not align well with the truth. These events should be analyzed further to determine if the width of the truth bounding box should be increased slightly. Other sources of false alarms include vertical wind shears, incorrectly dealiased velocities, noisy velocity fields, and contamination by out-of-trip weather, which produce a false convergence signature. Failures of the velocity dealiasing and out-of-trip weather removal are expected with the TDWR system. However, they do result in an increase in the gust front PFA.

An improved gust front detection algorithm known as the Machine Intelligent Gust Front Algorithm (MIGFA; Troxel and Delanoy, 1994) uses techniques to improve overall algorithm performance. MIGFA was run on the same cases as the TDWR algorithm to generate the results provided in Table 11.

The total number of gust fronts (the denominator in the POD statistic) used in the MIGFA analysis differs from the TDWR analysis because the scoring software does not allow the user to specify the beginning and end times of the data to be analyzed. The scoring software compares all detections in the algorithm output file to the truth database. The algorithm output files may start at slightly different times. (*e.g.*, Due to a need to "ramp up," MIGFA may not start generating results until a few time steps into the analysis period.) The scoring software recognizes which time steps are not analyzed by the algorithm and does not score those time steps. As a result, the number of gust fronts used in the analyses may differ. However, as long as the number of gust fronts used in the analyses are comparable, the probabilities can be used to compare the two algorithms.

A comparison of Table 10 and Table 11 shows that MIGFA detects gust fronts significantly better than the TDWR algorithm; both in POD and PLD. The PLD for MIGFA (all sites) is about 2.5 times greater than TDWR (*i.e.*, 70.8 versus 28.2 percent). This is an extremely significant improvement in gust front detection length probability. The main reasons for the differences are: (1) MIGFA uses a lower convergence threshold and (2) MIGFA combines evidence of the presence of gust fronts from both the reflectivity and Doppler velocity fields. As shown in Table 10 and Table 11, most of the improvement is in the weak and moderate intensity categories. There is only a slight difference in PLD for the fronts categorized as strong. MCO and MEM account for most of the increase in PLD, with the difference in MCO due primarily to the contribution from weak gust fronts.

## Table 11

### Machine Intelligent Gust Front Algorithm Performance Statistics

| Strength | POD (percent) | PFA (percent) | PLD (percent) | PFD (percent) |
|---|---|---|---|---|
| | | **DCA** | | |
| Weak | (169/238) 71.0 | - | (3738/6813) 55.6 | - |
| Moderate | (89/97) 91.8 | - | (3762/5055) 74.5 | - |
| Strong | (11/13) 84.6 | - | (597/889) 67.1 | - |
| All DCA | (269/348) 77.3 | (87/528) 16.5 | (8097/12757) 63.8 | (3756/17257) 21.8 |
| | | **MCO** | | |
| Weak | (639/726) 88.0 | - | (20214/27272) 74.1 | - |
| Moderate | (38/38) 100.0 | - | (1121/1351) 83.1 | - |
| All MCO | (677/764) 88.6 | (153/1571) 9.7 | (21335/28623) 74.5 | (9930/52891) 18.8 |
| | | **MEM** | | |
| Weak | (603/749) 80.5 | - | (17232/24767) 69.6 | - |
| Moderate | (144/160) 90.0 | - | (4095/5683) 72.1 | - |
| Strong | (48/50) 96.0 | - | (1632/2164) 75.5 | - |
| All MEM | (795/959) 82.9 | (258/1703) 15.1 | (22959/32614) 70.4 | (14895/53914) 27.6 |
| All Weak | (1411/1713) 82.3 | - | (41184/58852) 70.0 | - |
| All Moderate | (271/295) 91.9 | - | (8978/12089) 74.3 | - |
| All Strong | (59/63) 93.7 | - | (2229/3053) 72.8 | - |
| All Sites | (1741/2071) 84.1 | (498/3802) 13.1 | (52391/73994) 70.8 | (28581/124062) 23.0 |

The PFA for the TDWR algorithm is about three percent less than MIGFA (*i.e.*, 10.5 percent versus 13.1 percent), while the overall TDWR PFD (all sites) is about 50 percent better than MIGFA (15.1 percent for TDWR versus 23.0 percent for MIGFA). The MIGFA PFD is higher at all three sites. This is especially true for MCO and MEM.

The false detections from MIGFA were analyzed in more detail to ascertain the cause for the performance degradation. The increase in PFA is not proportional to the increase in PFD. Thus, MIGFA is not generating many more new detections, but is extending the lengths of valid fronts into regions of noisy data. Detections of vertical wind shear are another source of false alarms. Vertical wind shear (winds increasing with altitude) produces an apparent convergence signature in the Doppler velocity field. The TDWR algorithm requires the detection of a signature on the 0.5° and 1.0° scans (commonly referred to as vertical continuity). MIGFA does not require vertical continuity so it more susceptible to false alarms from vertical wind shear. This was a problem in the two April MEM cases. Other factors that caused MIGFA false alarms were noisy velocity data, range folding errors, and velocity dealiasing errors. The number of MIGFA false alarms due to velocity dealiasing failures has been dramatically reduced by recent modifications to negate the velocity data in those range gates that showed radical changes across the unambiguous velocity boundary. Based on the performance results described in this report, the MIGFA algorithm developers are investigating new techniques to reduce false events while still maintaining a high probability of detection.

# 6. RECOMMENDATIONS

Based on the findings reported herein, it is recommended that the following actions be taken to improve the performance of the TDWR system:

1. The VIL test should be evaluated by the TDWR Program Support Facility as a means to further reduce the microburst/wind shear PFA, which may approach the 10 percent threshold even with the 5B software.

2. Resources permitting, the gust front algorithm should be replaced with the MIGFA algorithm.

3. Data quality problems such as range aliasing, velocity aliasing and noise contamination should be investigated in detail to determine methods for the mitigation of these problems.

4. The scan mode switching criteria should be thoroughly evaluated to determine why the radar switches modes on reflectivity values below the threshold.

# REFERENCES


Klingle-Wilson, D., M. Donovan, S. Olson, and F. W. Wilson, 1992: A comparison of the performance of two gust front detection algorithms using a length-based scoring technique, Project Report ATC-185, DOT/FAA/NR-92/1, MIT Lincoln Laboratory, Lexington, MA.

Merritt, M. W., D. Klingle-Wilson, and S. Campbell, 1989: Wind Shear Detection with Pencil-Beam Radars, *The Lincoln Laboratory Journal*, v. 2(3), pp. 483-510.

Troxel, S., and R. L. Delanoy, 1994: Machine Intelligent Approach to Automated Gust Front Detection for Doppler Weather Radars, SPIE Proceedings - Sensing, Imaging, and Vision for Control and Guidance of Aerospace Vehicles, V. 2220, Orlando, FL, pp. 182-192.

Vasiloff, S., 1993: Terminal Doppler Weather Radar (TDWR) Operational Text and Evaluation: Final Report on Weather Detection Performance, NSSL Storm-scale Research and Applications Division, Norman, OK.

# LIST OF ACRONYMS

| | |
|---|---|
| AGL | Above Ground Level |
| AP | Anomalous Propagation |
| BDD | Base Data Display |
| CAR | Clear Air Reflectivity |
| CREM | Clutter Residue Editing Map |
| DCA | Washington National Airport |
| DFU | Display Functional Unit |
| MCO | Orlando International Airport |
| MEM | Memphis International Airport |
| MIGFA | Machine Intelligent Gust Front Algorithm |
| MTS | Moving Target Simulator |
| PRF | Pulse Repetition Frequency |
| PRI | Pulse Repetition Interval |
| RPG | Radar Product Generator |
| SNR | Signal-to-Noise Ratio |
| TDWR | Terminal Doppler Weather Radar |
| VIL | Vertically Integrated Liquid Water |

# APPENDIX
## Monitor Mode and Hazardous Mode Scan Strategies for the DCA TDWR

| Tilt Number | Monitor Mode | | Hazardous Mode | |
|---|---|---|---|---|
| | Elevation Angle | Scan Type | Elevation Angle | Scan Type |
| 1 | 0.6 | 360-degree scan; low PRF[1] for PRF selection | 0.6 | 360-degree scan; low PRF for PRF selection |
| 2 | 0.3 | 360-degree scan; PRF for velocity dealiasing | 0.3 | 360-degree scan; PRF for velocity dealiasing |
| 3 | 0.3 | 360-degree scan; used for gust front and microburst detection and velocity dealiasing | 0.3 | 360-degree scan; used for gust front and microburst detection and velocity dealiasing |
| 4 | 1.0 | 360-degree scan; used for gust front detection | 3.1 | sector scan |
| 5 | 3.1 | 360-degree scan; used for terminal precipitation | 6.2 | sector scan |
| 6 | 6.1 | 360-degree scan | 9.2 | sector scan |
| 7 | 11.0 | 360-degree scan | 12.2 | sector scan |
| 8 | 15.9 | 360-degree scan | 15.1 | sector scan |
| 9 | 20.8 | 360-degree scan | 17.9 | sector scan |
| 10 | 25.7 | 360-degree scan | 21.3 | sector scan |
| 11 | 30.6 | 360-degree scan | 0.3 | sector scan; used for microburst detection |
| 12 | 35.5 | 360-degree scan | 1.0 | 360-degree scan; used for gust front detection |
| 13 | 40.4 | 360-degree scan | 25.2 | sector scan |
| 14 | 45.3 | 360-degree scan | 29.5 | sector scan |
| 15 | 50.2 | 360-degree scan | 34.3 | sector scan |
| 16 | 55.1 | 360-degree scan | 39.4 | sector scan |
| 17 | 60.0 | 360-degree scan | 0.3 | sector scan; used for microburst detection |
| 18 | | | 3.1 | 360-degree scan; used for terminal precipitation |
| 19 | | | 6.2 | sector scan |

## Monitor Mode and Hazardous Mode Scan Strategies for the DCA TDWR (Continued)

| Tilt Number | Monitor Mode | | Hazardous Mode | |
|---|---|---|---|---|
| | Elevation Angle | Scan Type | Elevation Angle | Scan Type |
| 20 | | | 9.2 | sector scan |
| 21 | | | 12.2 | sector scan |
| 22 | | | 15.1 | sector scan |
| 23 | | | 0.3 | sector scan; used for microburst detection |
| 24 | | | 17.9 | sector scan |
| 25 | | | 21.3 | sector scan |
| 26 | | | 25.2 | sector scan |
| 27 | | | 29.5 | sector scan |
| 28 | | | 34.3 | sector scan |
| 29 | | | 39.4 | sector scan |
| 30 | | | 1.1 | sector scan |
| 31 | | | 0.3 | sector scan; used for microburst detection |